

Nickel incorporated into Anodic Porous Alumina formed on an Aluminium Wire

Nobuyuki Ohji, Nobuhito Enomoto, Takanori Mizushima and Noriyoshi Kakuta

Department of Materials Science, Toyohashi University of Technology, Tempaku, Toyohashi, Aichi 441, Japan

Yoshio Morioka and Akifumi Ueno*

Faculty of Engineering, Shizuoka University, Johoku, Hamamatsu, Shizuoka 432, Japan

Porous alumina films have been prepared on the surface of an aluminium wire by anodic oxidation in an oxalic acid electrolyte. The pore size could be controlled by the anode potential, and the thickness of the alumina film was a function of the anodizing time as well as the anode potential used. Silica powders containing finely divided Ni metal particles were incorporated into the micropores of the alumina films, which were then used as wire catalysts. The wire catalyst did not require any supplementary heating during catalytic reactions, since after 1 min of applying a small voltage across the ends of the wire, a temperature of 573 K could be reached. The catalytic performance of the nickel particles mounted in the aluminium wires for the hydrogenation of but-1-ene was measured and compared with that of a conventional supported-nickel catalyst.

Since the proposal of hexagonal pillar cells by Keller *et al.*¹ as a model for the micropores formed on anodic aluminium films, the morphology and mechanism of pore formation on anodic alumina films have been of considerable interest in the fields of corrosion and surface modification science and technology. Takahashi *et al.*² and Furneaux *et al.*³ have developed techniques for direct observation of these hexagonal pillar cells by transmission electron microscopy using an ultramicrotome for the preparation of the sample specimen, resulting in more precise measurements of the cell sizes and the pillar heights of the anodic films.

On the basis of these measurements, the nucleation and growth of the porous anodic films on aluminium, prepared in various electrolytes, have been extensively discussed by Thompson *et al.*^{4–6} They reported that the local field strengths across the oxide (barrier) layers, varying with the electrolyte employed, control the steady-state anodizing behaviour observed in the acidic electrolytes under conditions of constant voltage.⁷

In contrast, the application of these porous anodic films to novel functional materials has been of interest in the fields of magnetic data storage^{8,9} and catalysis,¹⁰ since these pores could work as nanotemplates for incorporation of small metal and/or metal oxide particles.¹¹ In these studies, the method of incorporation of the small metal and/or metal oxide particles into the micropores formed on the anodic films is the key technique. In this work, anodic aluminas formed on an aluminium wire were immersed in sols consisting of ethyl silicate and nickel nitrate dissolved in ethylene glycol,¹² where nickel ions were trapped in the $-\text{Si}-\text{O}-\text{Si}-$ nets of the silica sols forming an $-\text{Si}-\text{O}-\text{Ni}-\text{O}-\text{Si}-$ structure. After reduction of the calcined aluminium wire in flowing hydrogen, some of the finely divided nickel particles dispersed in the silica power were found to be incorporated into the micropores of the anodic alumina films on the aluminium wire. Some kinetic studies on the hydrogenation of but-1-ene were carried out using these wire catalysts at various temperatures. It was found that the reaction required the same activation energy as over a conventional supported-nickel catalyst.

Experimental

Preparation of Anodic Porous Alumina

Porous alumina films were prepared by anodizing an alu-

minium plate (40 mm × 30 mm × 0.23 mm) or a spiral aluminium wire (1 m × 0.25 mm od), both >99.99% purity obtained from Furukawa Electric Industry Co., at a voltage in the range 10–80 V in a 0.16 mol dm⁻³ oxalic electrolyte at 293 K using a graphite cathode and a regulator dc supply (Kikusui Denshi Co., PAD-110-5). The current observed was rapidly depressed in the first 10 s of anodizing, and then gradually increased to a constant value (165 mA for a plate and 51 mA for a wire at 50 V, respectively) within 100 s. Unless otherwise specified, anodizing was continued for 10 min at constant voltage. The porous alumina films formed on the aluminium plates were dried and calcined at 623 K for 1 h, and then placed in a high-resolution scanning electron microscope (SEM, Hitachi S-900), operated at an accelerating voltage of 5 kV, in order to measure the open pore sizes and the film thicknesses (pillar heights), respectively. Since SEM observations of the porous films on the aluminium wires was difficult, the pore sizes and film thicknesses on the spiral wires were postulated to be the same as those observed on the plates under the same anodic conditions.

Incorporation of Nickel-dispersed Silica into the Micropores

The anodic porous aluminas formed on the plates and/or wires, dried and calcined at 623 K in air for 1 h, were immersed in sols, prepared by hydrolysis of a mixture of ethyl silicate (30 cm³) and nickel nitrate (8.9 g) dissolved in ethylene glycol (150 cm³) with a small amount of nitric acid (2 cm³).¹² The sols consisted of silica colloids, trapping nickel ions in the $-\text{Si}-\text{O}-\text{Si}-$ nets forming an $-\text{Si}-\text{O}-\text{Ni}-\text{O}-\text{Si}-$ structure evidenced by extended X-ray absorption fine structure (EXAFS) measurements.¹³ The silica colloidal particles were roughly evaluated to be <10 nm in diameter on average.¹⁴ After immersion for 10 min at 298 K, the plates and/or wires were withdrawn at a pulling rate of 80 mm min⁻¹, followed by drying and calcining at 623 K for 4 h, and by reduction at 673 K for 1 h in flowing hydrogen. The formation of nickel metal particles in the porous alumina on an aluminium plate was posed by X-ray thin-film diffraction (Rigakudenki, RAD-5A), with an incident angle of 0.5 and a graphite slit system in front of a detector. A Cu tube was operated at 50 kV and 40 mA. In the present work, silica-coated wire catalysts were also prepared by immersing calcined anodic wires into a silica-sol solution consisting of ethyl silicate and a small amount of nitric acid.

The anodic alumina films formed on a plate were mounted in a resin and sliced by an ultra-microtome into thin films, which were immersed in an aqueous solution of mercury(II) chloride.¹⁵ The sliced alumina films were separated from the aluminium metal plate owing to the formation of an Hg–Al amalgam during the immersion. The alumina films separated from the aluminium plate were examined by transmission electron microscopy (TEM, Hitachi H-800 instrument) and electron probe microanalysis (EPMA, Horiba EDX Instrument, equipped with an energy-dispersive detector), in order to measure the shapes and sizes of the nickel metal particles and to estimate the amount of nickel metal loaded in the porous alumina films, respectively.

Catalytic Performance of the Wire Catalysts

Although the alumina films formed on aluminium wire were readily heated to 573 K in 1 min simply by loading a small voltage to the ends of the wire, the films formed on the plate were heated to at most 323 K, because of the low electric resistance between both sides of the plate. In order to measure the temperature of the alumina films, a thermocouple was attached to the wire surface using a heat-resistant resin, although temperatures > 573 K could not be measured precisely.

Hydrogenation of but-1-ene to butane was carried out at 358, 388 and 419 K using a closed-circulation system, equipped with a cylindrical glass reactor possessing two copper electrodes to which each end of the wire catalyst was connected to be heated electrically. Besides butane, butene isomers such as (*E*)- and (*Z*)-but-2-ene were detected during the reaction by gas chromatography using a column packed with VZ-7. The initial pressures of hydrogen and but-1-ene were both 53 kPa, and the rate constants for the formation of butane were estimated assuming the following rate equation:

$$d(P_{\text{butane}})/dt = k(P_{\text{but-1-ene}})^{0.5}(P_{\text{H}_2})^{0.5.16}$$

For comparison, supported-Ni catalysts were prepared by immersing alumina powders in sols formed from hydrolysis of a mixture of ethyl silicate and Ni nitrate dissolved in ethylene glycol, whose compositions were described above. The catalyst was then dried, calcined and reduced in flowing hydrogen in the same manner as mentioned above. The loading of Ni metal in the catalyst prepared was 2.0 wt.%, measured by X-ray fluorescence spectroscopy after extraction of the Ni ions with hot nitric acid, whereas the amount of Ni

ions in the alumina films, separated from the aluminium plates, was roughly estimated to be 1.9 wt.% by EPMA measurements. The catalytic performance for the hydrogenation of but-1-ene was also studied in a similar manner to that applied to the wire catalysts.

Results

Characterization of Anodic Alumina formed on Aluminium Plates

The pore size, alumina film thickness and barrier layer of the anodic alumina films are defined in Fig. 1, where the Keller model for anodized porous alumina films is drawn. High-resolution SEM photographs of the porous anodic alumina formed on an aluminium plate held at 50 V for 10 min, followed by calcination at 623 K for 1 h in air, are given in Fig. 2(a) (plane view) and (b) (sectional view), where the open-pore sizes and the film thickness (pillar heights) were measured. In Fig. 3 are shown the changes in average pore size and film

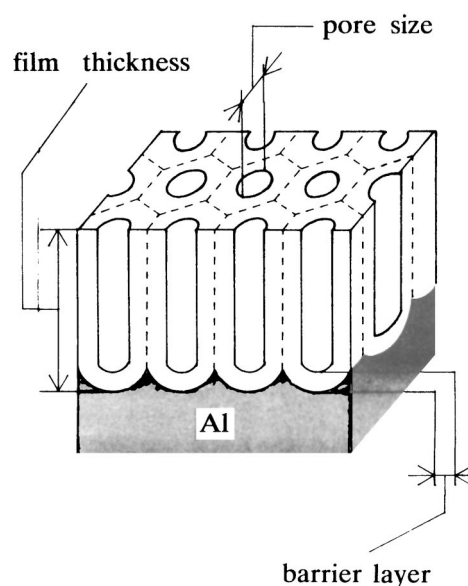


Fig. 1 Keller model for the anodic porous alumina films, showing the definitions of pore size, film thickness and barrier layer

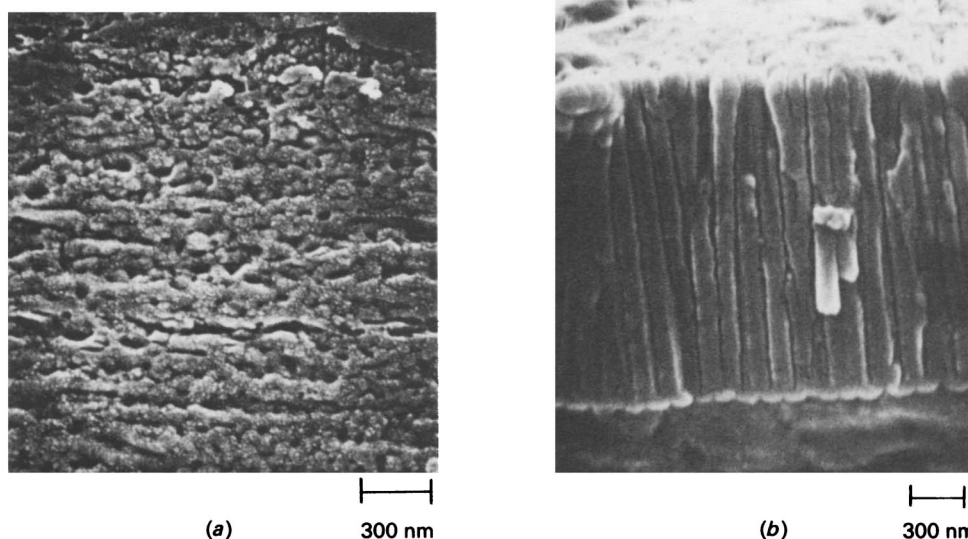


Fig. 2 SEM photographs of anodic alumina films: (a) plane view and (b) sectional view of the alumina films formed on the aluminium plate

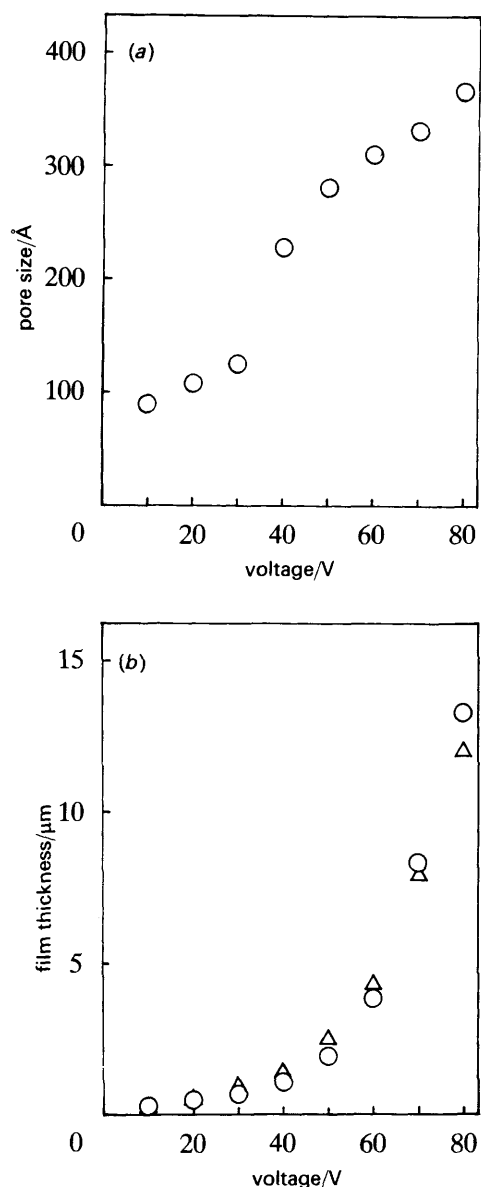


Fig. 3 Relationships between the voltage applied to the aluminium plate and (a) the pore size and (b) the alumina film thickness: (○) experimentally and (△) theoretically observed

thickness on the aluminium plates anodized at various voltages for 10 min. Film thicknesses calculated from the following equation are also given in Fig. 3:¹⁷

$$h = \frac{Mit}{6Fd}$$

where h is the film thickness, M is the molecular weight of alumina, I is the current observed during steady-state anodizing, t is the anodizing time, F is the Faraday constant and d is the current density at the aluminium surface. The apparent surface area of the aluminium plate used in this work is 24.3 cm² (see Table 1) and the anodizing time is 10 min. The current during steady-state anodizing varied with the anode potential used (see Fig. 4). From the equation above, the film thickness should be proportional to the anodizing time under conditions of constant current. The results obtained at a constant voltage (50 V), and hence at a constant current (165 mA), are given in Fig. 5. In Table 1 the apparent surface area, the current during steady-state anodizing under 50 V, and the current density at the surface of the aluminium plate are

Table 1 Apparent surface areas, currents during steady-state anodizing at 50 V, and the current densities on the aluminium plate and wire

	apparent surface area /cm ²	current value /mA	current density /mA cm ⁻²
Al plate	24.32	165.0	6.78
Al wire	7.62	51.0	6.70

compared with the corresponding values for the aluminium wire.

Ni Metal Particles in the Porous Alumina Films of Aluminium Plates

High-resolution SEM photographs of the reduced porous alumina on an aluminium plate are shown in Fig. 6(a) (plane)

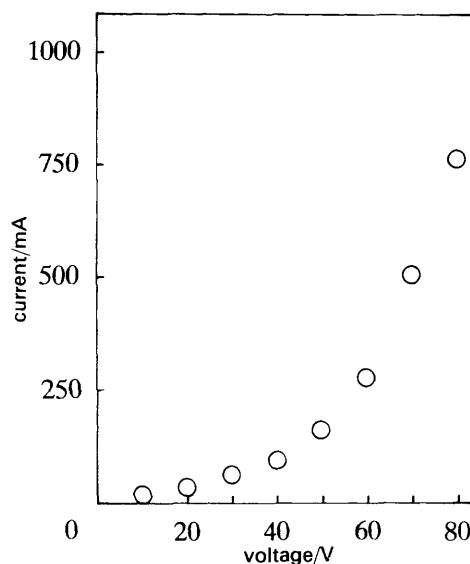


Fig. 4 Variation in current during steady-state anodizing with applied voltage on the aluminium plate

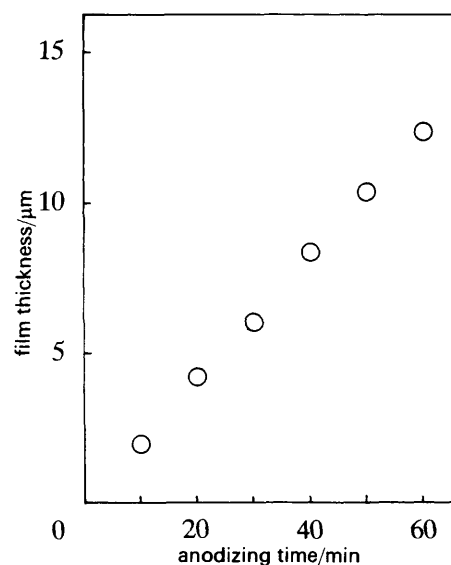


Fig. 5 Linear relationship between alumina film thickness and the anodizing time

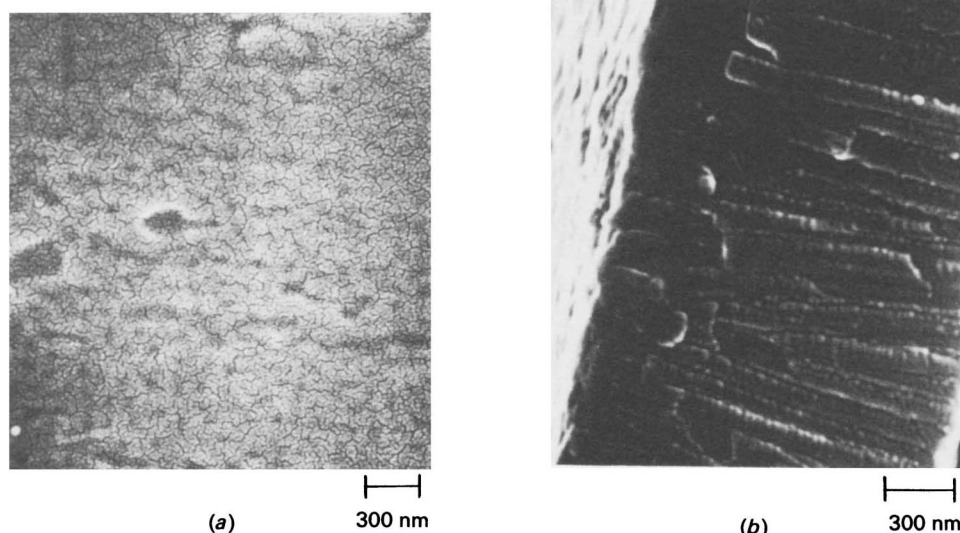


Fig. 6 SEM photographs of the hydrogen-reduced alumina films on the aluminium plate. Silica-supported nickel particles were dispersed onto the alumina films: (a) plane view and (b) sectional view.

and (b) (sectional view), where the alumina surface was completely covered with a nickel-containing silica film. It was also noted from Fig. 6(b) that small-grain silica powders, probably including nickel metal particles, were deposited on

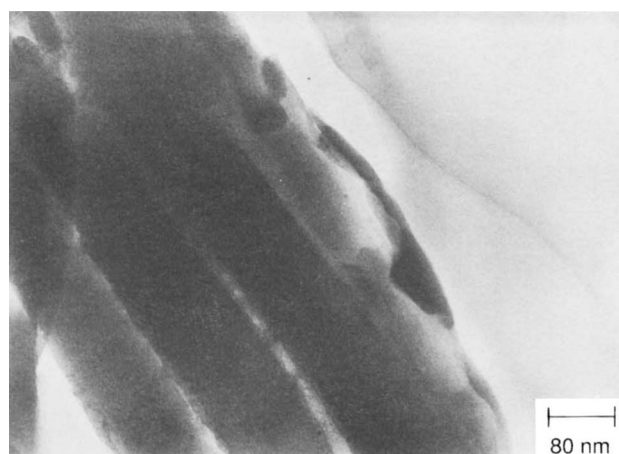


Fig. 7 TEM photograph of nickel or nickel oxide particles dispersed inside the pores of alumina films formed on the aluminium plate

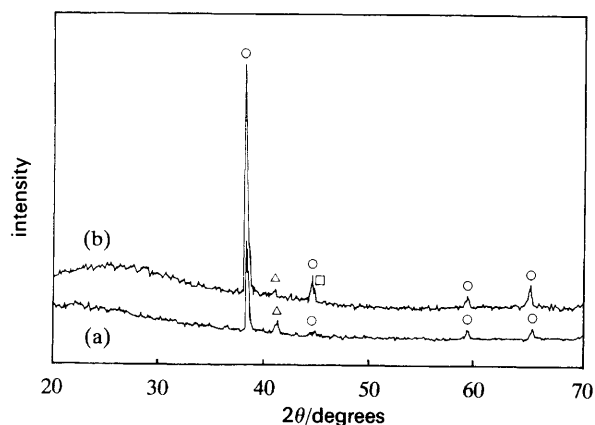


Fig. 8 X-Ray thin-film diffractions of the calcined (a) and reduced (b) alumina films formed on the aluminium plate. Silica-supported nickel and nickel oxide particles were in the alumina films. (○) Al, (△) NiO, (□) Ni.

the pore walls of the alumina films. Fig. 7 shows a TEM photograph of the reduced alumina films separated from the aluminium plate, where the formation of nickel metal particles, or nickel oxide crystallites, in the micropores of alumina films is evidenced. X-Ray thin-film diffractions of both the calcined and reduced alumina films are given in Fig.

Table 2 Conversion and selectivity observed on the wire catalyst for the hydrogenation of but-1-ene at 419 K for 24 h

catalyst	conversion (%)	selectivity (%)		
		butane	(Z)-but-2-ene	(E)-but-2-ene
wire catalyst	27.9	37.9	40.0	22.1
wire catalyst without Ni	0.07	trace	trace	trace

Reaction carried out at 419 K.

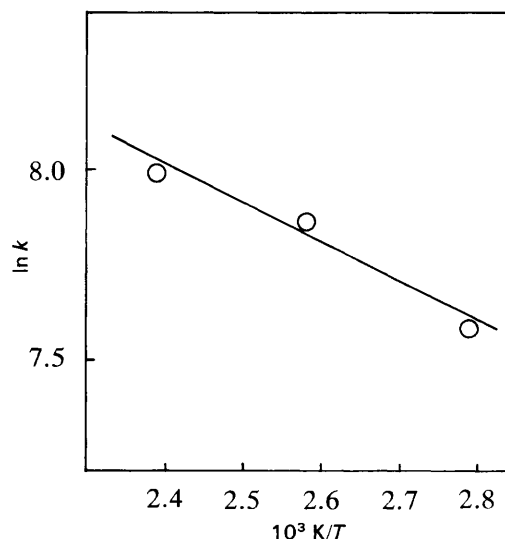


Fig. 9 Arrhenius plot of the rate constants for the hydrogenation of but-1-ene on the wire catalyst; $E_a = 2.3 \text{ kcal mol}^{-1}$

8, which suggests that nickel metal particles and/or the oxides are deposited on the surface of the alumina films as well.

Hydrogenation of But-1-ene over Ni-dispersed Wire Catalysts

Each end of the wire catalyst (1 m) was connected to the copper electrode mounted in the glass reactor. Prior to the introduction of the H₂-but-1-ene gas mixture into the reactor, the catalyst was re-reduced by passing a current of 2 A through it under an H₂ atmosphere (corresponding to heating the catalyst to 523 K), followed by evacuation at the same temperature. The hydrogenation of but-1-ene on the wire catalyst was carried out at 419, 388 and 358 K, which corresponds to passing currents of 1.5, 1.3 and 1.1 A, respectively, through the wire catalyst, for 24 h. Gas samples were taken every 3 h during the reaction. Table 2 lists the results obtained after reaction for 24 h both on this wire catalyst and on the silica-dispersed (without Ni metal) wire catalyst. No reactions were observed on the silica-dispersed wire catalyst, suggesting that hydrogenation, as well as isomerization, of but-1-ene occurred on the Ni metal particles dispersed on the wire catalyst. The activation energy was 2.3 kcal mol⁻¹, calculated from the results shown in Fig. 9.

Discussion

Control of Pore Size and Film Thickness of the Anodic Alumina Films

The rapid decrease in current through the aluminium plate during the early stages of anodizing was due to the formation of alumina thin films on the plate surface, and the successive gradual increase in current was caused by the local dissolution of the alumina film into the solution of oxalic acid electrolyte. Under conditions of steady-state anodizing, equilibrium between the formation and dissolution of the alumina films on the aluminium plate was achieved.¹⁷ The pore size, which was rather smaller at the open pore [see Fig. 2(b)], was controlled only by the voltage applied between the aluminium plates and the graphite electrode, large pores with a large voltage and small pores with a small voltage, as depicted in Fig. 3. Although the nucleation mechanism has not yet been well defined, the pores were homogeneously generated over the plate surface, as can be seen in Fig. 2(a). The anodic film thickness was also a function of the applied voltage, and increased exponentially as the applied voltage increased, which was well reproduced by the theoretical curve obtained from the equation given above. A linear relationship between the oxide film thickness and the anodizing time at constant voltage and current (50 V and 165 mA) was observed (see Fig. 5), as predicted from the equation. Considering the fact that the pore size was constant at any part of the pore, except at an open pore [see Fig. 2(b)], this suggests that the dissolution of alumina predominantly occurred at the bottom of the pores (barrier layer) during the steady-state anodizing, and hence, the growth rate of the anodic alumina films might be a function of the local field strength across the barrier layer.⁶

As can be seen in Fig. 4, the current passing through the aluminium plate during steady-state anodizing also increased exponentially as the applied voltage increased, which is almost the same as the relationship between the oxide film thickness and applied voltage (see Fig. 3). The major factor controlling film thickness is, however, not the current itself but the current density (d), as expressed in the equation. The current densities were calculated from the currents observed during steady-state anodizing (see Fig. 4) and the apparent

surface area of aluminium electrode employed (see Table 1). Therefore, the current density through the aluminium plate was almost the same as that through the aluminium wire used here, suggesting that the relationship between the alumina film thickness and the applied voltage on the aluminium plate, given in Fig. 3, might be the same as the corresponding relationship for the aluminium wire. The pore size, however, is controlled only by the applied voltage for both the plate and the wire.

Characterization of Ni Metal Particles dispersed in the Anodic Alumina Films

Because of the repulsive forces caused by the electric double layer around alumina, metal cations cannot approach the alumina surface in acidic solution,¹⁸ which makes it difficult to deposit metal or metal oxide particles on the alumina surface, especially on the pore walls of the anodic alumina films. In most cases, electrodeposition was carried out using an aqueous solution of the metal salts of interest, buffered with boric acid.^{9,19} In the present work, the calcined anodic aluminium plate and wire were immersed in silica sols containing Ni ions in their net frameworks as —Si—O—Ni—O—Si— structures, which might not be affected by the repulsive forces around alumina, since these macromolecules are neutral.¹⁴ It was further confirmed that Ni ions were released from the sol nets and migrated into the pores of the alumina films when these macromolecules were adsorbed by the alumina surface, leaving silica layers on the surface of the alumina films.¹⁴

As can be seen in Fig. 8, nickel oxide crystallites were actually formed in the alumina films on the aluminium plate and some of the oxide crystallites were reduced by hydrogen to nickel metal particles. Because of the low melting point of aluminium, the reduction was carried out at 673 K, which is not high enough to reduce all of the nickel oxide crystallites to metal. The open pores observed on the surface of the calcined alumina films [see Fig. 2(a)] were completely covered with a layer of silica, probably containing nickel and nickel oxide crystallites [see Fig. 6(a)], although a lot of cracks and holes were noted on the silica layer. Silica deposition was also confirmed inside the pores, as shown in Fig. 6(b). Since it was difficult to distinguish nickel particles from the silica deposits in these SEM photographs, the alumina films were separated from the aluminium plate and subjected to TEM observation. A few small black spots, not so clear, can be seen in the TEM photograph, shown in Fig. 7. These spots are probably nickel or nickel oxide crystallites, about 50 Å in diameter, deposited inside the pores. Judging from the number of particles inside the pores, most of the metal and metal oxide particles were, however, in the silica layer covering the alumina surface, which is different from the results obtained in our previous work.¹⁴ This difference can be ascribed partly to the differences in the amounts and strengths of acid sites on the alumina surfaces. Many strong acid sites were present on the surface of the alumina (spheres), assisting the Ni ions to leave the net framework of the silica sol.

Catalytic Performance for the Hydrogenation of But-1-ene

Although most of the metal and metal oxide particles were found in the silica layer formed on the alumina surface, the aluminium wire containing nickel metal particles was used as a catalyst for the hydrogenation of but-1-ene at 419, 388 and 358 K, respectively. These temperatures were achieved by passing current of 1.5, 1.3 and 1.1 A, respectively, through the

wire catalyst. As can be seen in Table 2, hydrogenation to butane and isomerization to (*E*)- and (*Z*)-but-2-ene took place over the wire catalyst, but not over the wire without nickel particles. It was also of interest to see if the current passed could have any effects upon the catalytic performance of the nickel, since the nickel metal particles were located so close to the aluminium wire that the local electric fields across the alumina films were expected to play some role in the catalytic properties of the metal. The activation energy for the hydrogenation of but-1-ene to butane on the wire catalyst was estimated to be 2.1 kcal mol⁻¹ (see Fig. 9), which is very close to the values of 2.0 and 2.5 kcal mol⁻¹, reported by Dibeler and Taylor²⁰ and by Twigg,¹⁶ respectively. For comparison, alumina-supported nickel catalysts, prepared in the present work, were applied to the hydrogenation of but-1-ene in the same temperature range, resulting in an activation energy of 2.3 kcal mol⁻¹. These results indicated that there are no effects of local electric fields on the catalytic performance of nickel metal particles dispersed in the wire catalyst, although further details, such as the turnover frequency on a nickel atom, have not been evaluated in the present work.

This work was supported by Grants-in-Aid for scientific research from the Ministry of Education, Science and Culture of Japan.

References

- 1 F. Keller, M. S. Hunter and D. L. Robinson, *J. Electrochem. Soc.*, 1953, **100**, 411.

- 2 H. Takahashi, M. Nagayama, H. Akahori and A. Kitahara, *J. Electron. Microsc.*, 1973, **22**, 149.
- 3 R. C. Furneaux, G. E. Thompson and G. C. Wood, *Corros. Sci.*, 1978, **18**, 853.
- 4 G. E. Thompson, R. C. Furneaux and G. C. Wood, *Trans. Inst. Metal Finish.*, 1977, **55**, 117.
- 5 G. E. Thompson, R. C. Furneaux and G. C. Wood, *Trans. Inst. Metal Finish.*, 1978, **56**, 159.
- 6 G. E. Thompson, R. C. Furneaux, G. C. Wood, J. A. Richardson and J. S. Goode, *Nature (London)*, 1978, **272**, 43.
- 7 G. E. Thompson and G. C. Wood, *Nature (London)*, 1981, **290**, 230.
- 8 D. AlMawlawi, and M. Moskovits, *J. Appl. Phys.*, 1991, **70**, 4421.
- 9 C. K. Preston and M. Moskovits, *J. Phys. Chem.*, 1993, **97**, 8495.
- 10 N. Nourbakhsh, B. J. Smith, I. A. Webster, J. Wei and T. T. Tsotsis, *J. Catal.*, 1991, **127**, 178.
- 11 D. G. Goad and M. J. Moskovits, *J. Am. Chem. Soc.*, 1989, **111**, 9250.
- 12 A. Ueno, H. Suzuki and Y. Kotera, *J. Chem. Soc., Faraday Trans. 1*, 1983, **79**, 127.
- 13 K. Tohji, S. Tanabe, Y. Udagawa and A. Ueno, *J. Am. Chem. Soc.*, 1984, **106**, 612.
- 14 T. Fujiyama, M. Ohtsuka, H. Tsuiki and A. Ueno, *J. Catal.*, 1987, **104**, 323.
- 15 S. Wernick, *J. Electrodep. Tech. Soc.*, 1934, **9**, 153.
- 16 G. H. Twigg, *Proc. R. Soc., London, Ser. A*, 1941, **178**, 106.
- 17 M. Nagayama and H. Takahashi, *Nippon Kagaku-Kaishi*, 1972, 850.
- 18 H. R. Kruyt, *Colloid Science*, Elsevier, Amsterdam, 1948, vol. 1.
- 19 T. J. Marks, *Science*, 1985, **227**, 881.
- 20 V. H. Dibeler and T. H. Taylor, *J. Phys. Chem.*, 1951, **55**, 1036.

Paper 3/07474I; Received 20th December, 1993